

NATIONAL ADVISORY COMMITTEE FOR AERONAUTICS

TECHNICAL NOTE 4051

EFFECTS OF RAPID HEATING ON STRENGTH OF AIRFRAME COMPONENTS

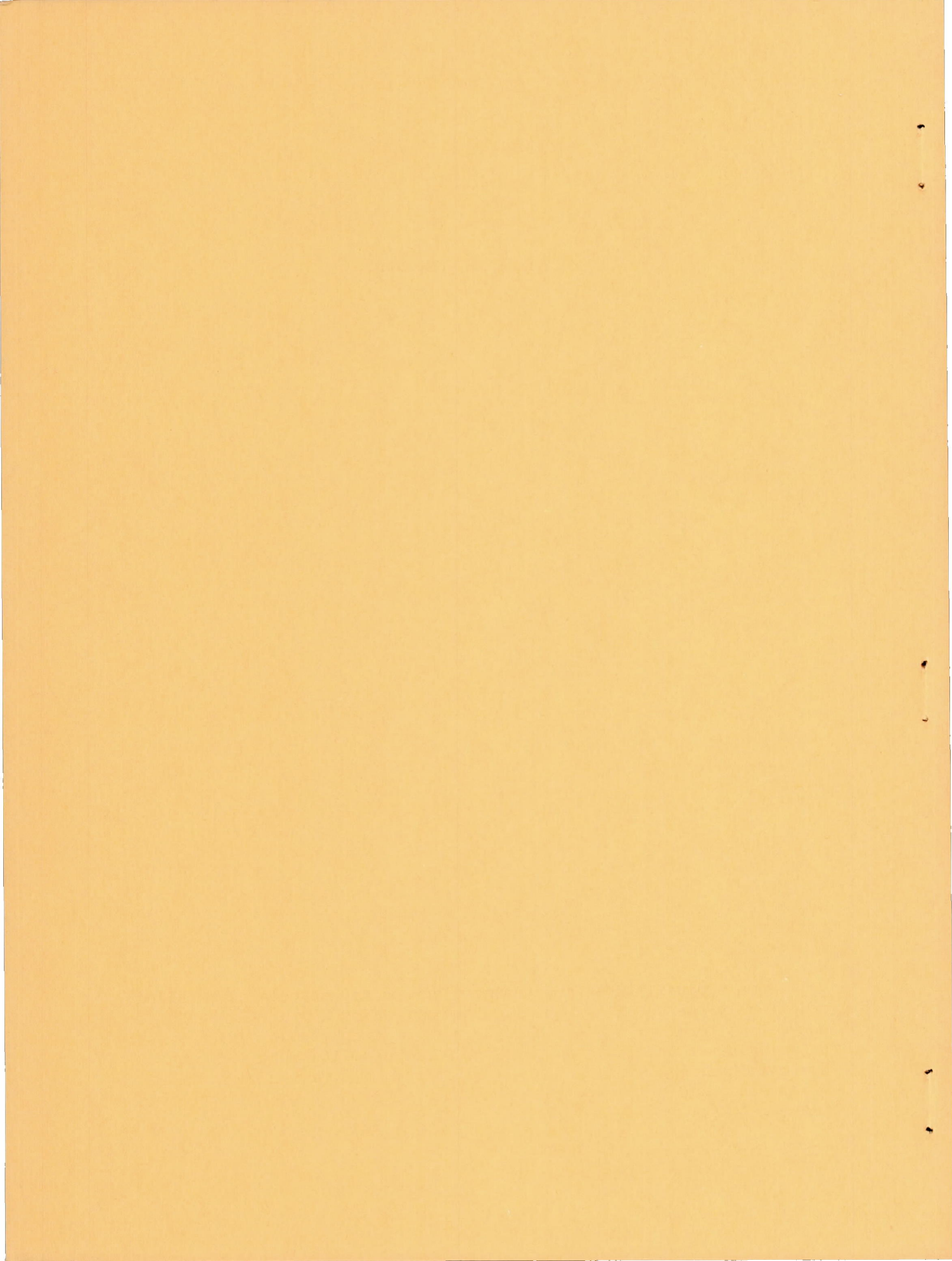
By Richard A. Pride, John B. Hall, Jr.,
and Melvin S. Anderson

Langley Aeronautical Laboratory
Langley Field, Va.



Washington

June 1957



TECHNICAL NOTE 4051

EFFECTS OF RAPID HEATING ON STRENGTH
OF AIRFRAME COMPONENTSBy Richard A. Pride, John B. Hall, Jr.,
and Melvin S. Anderson

SUMMARY

Results of several experimental investigations are presented which indicate the effects of rapid heating on the bending strength of multiweb beams and ring-stiffened cylinders. It is shown that thermal stresses reduce the bending load carried at buckling by both beams and cylinders. The influence of thermal stress on maximum load is found to depend largely on the mode of buckling. For beams that buckle locally, no apparent effect of thermal stress on the maximum load has been found. A reduction in maximum load has been observed for beams that buckle in the wrinkling mode and for cylinders.

INTRODUCTION

Aerodynamic heating rates currently contemplated in airplanes and missiles may impose severe thermal stresses on primary structures. This paper considers the influence of such thermal stresses on the bending strength of multiweb beams and ring-stiffened cylinders.

Observation of the behavior of various types of structures under combinations of loads and thermal stresses has indicated that the effect of thermal stress on buckling is to reduce the bending load which may be carried prior to buckling and that the effect of thermal stress on maximum load may be correlated with the type of stress-shortening diagram of the structure.

Some typical stress-shortening diagrams and associated buckling modes are presented in figure 1. Local buckling has a stress-shortening curve that permits considerable increase in both stress and shortening to occur after buckling and prior to failure. Within this region of increasing stress and shortening, it is possible that a redistribution of stress would alleviate the detrimental effect of thermal stress on maximum load.

In contrast, the stress-shortening curve for a structure such as a ring-stiffened cylinder usually drops abruptly after buckling (fig. 1). Hence, a reduction in buckling stress produced by thermal stress should be reflected as a corresponding loss in maximum strength. A stress-shortening diagram in which considerable shortening occurs for negligible increase in stress exists for structures such as multiweb beams with formed-channel webs which buckle in a mode known as wrinkling. This mode is characterized by buckles extending across the chord of the beam. The considerable shortening that can occur after buckling indicates that some influence of thermal stress on failure may be anticipated; however, this influence may not be as great as for the cylinder.

Tests to explore thermal-stress effects on the bending strength of these three types of structures have been made and some of the results are presented in preliminary form in this paper.

SYMBOLS

| | |
|-------|---|
| A | cross-sectional area, sq in. |
| b | plate width, in. |
| c | distance from neutral axis to center of skin, in. |
| E | Young's modulus, ksi |
| E_B | secant modulus for bending stress in skin, ksi |
| E_S | secant modulus for skin, ksi |
| E_W | secant modulus for web, ksi |
| I | moment of inertia, in. ⁴ |
| k | plate buckling coefficient |
| l | cylinder ring spacing, in. |
| M | bending moment, in-kips |
| r | cylinder radius, in. |
| s | peripheral distance, in. |

| | |
|----------------|---|
| T | temperature, °F |
| \bar{T} | average temperature, °F |
| \dot{T} | temperature rate with respect to time, °F/sec |
| t | plate thickness, in. |
| α | coefficient of thermal expansion, per °F |
| η | plasticity reduction factor |
| σ | stress, ksi |
| $\bar{\sigma}$ | average stress, ksi |
| μ | Poisson's ratio |

Subscripts:

| | |
|----|--------------------------------------|
| B | bending |
| cr | critical |
| cy | 0.2-percent-offset compressive yield |
| f | failure |
| S | skin |
| W | web |

BEAM STRENGTH

The test setup for applying both bending loads and rapid heating on beams is shown in figure 2. A one-cell beam is shown supported on columns about one-third the distance from each end and loaded in bending by the hydraulic jacks at the ends. Rapid heating is applied to the top and bottom skins of the beam by means of high-intensity quartz-tube lamp radiators located behind the reflectors. Strain gages and deflection pickups mounted on the cold webs give an indication of overall beam behavior during the test.

Failure Associated With Local Buckling

A large number of tests have been made on one-cell beams that buckle in the local mode. A representative temperature distribution around the cross section is shown in figure 3 for a beam 7.35 inches square with a wall thickness of 0.152 inch. The variation of temperature with peripheral distance for one quadrant of the beam is shown. For the maximum heating time in these tests, the temperature of the center of the skin rises to about 600° F, while the temperature of most of the webs rises to only about 100° F. Temperature distributions such as this will produce large thermal stresses in these beams.

For these aluminum-alloy beams, skin temperatures in the range from 400° to 600° F also produce deterioration in the material properties. In order to separate the loss in beam strength caused by deterioration of material properties from the loss in beam strength caused by thermal stress, a different type of test was made in which all sides of the beam were uniformly heated at a high rate. The test results for local buckling of these one-cell beams are shown in figure 4. The bending load stress in the skin of the beam is plotted against the average skin temperature. For the uniform heating case the skin temperature is the average temperature around the entire beam cross section; whereas, the average skin temperature is indicated for the nonuniform heating case in which the skins are heated at about 100° F/sec. For the nonuniform heating tests the existence of a difference in temperature between skins and webs is implied as was shown in figure 3.

Results are given in figure 4 for beams having two different values of width-thickness ratio for the skin; for one beam proportion buckling occurred in the elastic-stress range so that a large increase in stress after buckling was possible, and for the other beam proportion buckling occurred in the plastic range so that only a slight increase in stress beyond buckling was obtained. The upper curve for $b/t = 48$ gives the calculated buckling stress for uniformly heated beams and shows the effect of material deterioration on the elastic buckling stress. The buckling stress was determined from the following equation:

$$\sigma_{cr} = \frac{k\pi^2 \mu E}{12(1 - \mu^2)} \left(\frac{t_s}{b_s} \right)^2 \quad (1)$$

The slight reduction in buckling stress shown is the result of changes in elastic modulus with temperature. The open square test points in figure 4 are the confirming tests for this curve.

The lower curve for $b/t = 48$ determined from the following equation is the calculated amount of bending load stress required to produce buckling when thermal stress is present along with material deterioration:

$$\sigma_B = \sigma_{cr} - \frac{\alpha E_S (\bar{T}_S - \bar{T}_W)}{1 + \frac{E_S A_S}{E_W A_W}} \quad (2)$$

Equation (2) was developed in an earlier investigation (not generally available). The region between the two lower curves in figure 4 is a measure of the thermal stress as calculated by the last term in equation (2). The solid square test points indicate confirming tests for this elastic thermal-stress buckling condition.

For $b/t = 30$ the buckling stress is in the plastic range for this material. The upper curve in figure 4 gives the calculated effect of material deterioration on buckling stress for uniform heating. The buckling stress was again determined from equation (1) by using the plasticity reduction coefficient $\eta = E_S/E$. The lower curve gives the calculated amount of bending load stress required to produce buckling when both material deterioration and thermal stress are considered (eq. (2)). Again the region between these two curves represents the amount of thermal stress present at buckling. The tests are in agreement with the calculations. It should be noted that about one-half of the test results presented in figure 4 were obtained for beams that were loaded first and then heated, with the remaining beams heated first and then loaded. No discernable effects of sequence could be found.

Thus, it appears that local buckling of beams with integral webs can be predicted at elevated temperatures either with uniform heating or with temperature gradients, and in both the elastic and the plastic stress ranges.

The maximum strength of these same beams is given in figure 5. The curves show the maximum strength of the beams for uniform heating calculated from the following equation:

$$\bar{\sigma}_f = \frac{M_f c}{I} \quad (3)$$

where

$$M_f = 1.847 \sqrt{E_B \sigma_{cy}} t_S^2 b_W + 0.460 \sigma_{cy} b_W^2 t_W \quad (4)$$

Equation (4) was developed in another investigation (not generally available) and is dependent only on beam dimensions and material properties at elevated temperature. The calculated curves of figure 5 correspond to the same uniform heating case as the upper buckling curves for each value of b/t in figure 4. A considerable difference exists between the buckling stress and failure for $b/t = 48$. At $b/t = 30$ this difference in stress is practically gone as a result of plastic buckling; however, a considerable amount of beam deflection occurred between buckling and failure, even though the stress increased only slightly. The open test points corresponding to uniform heating indicate that the failure calculation is valid for both types of beams. The solid points represent test conditions at maximum load for the beams which had developed large thermal stresses at buckling. As indicated by the intermingling of the open and solid test points, no effect of thermal stress is evident on the maximum load. This result is equally true for beams that buckled either elastically or plastically.

Failure Associated With Wrinkling

The preliminary results obtained for a series of multiweb beams designed to aircraft proportions and fabricated from 17-7 PH stainless steel are given in figure 6. The interior structure consists of thin formed-channel webs riveted to the skins. In this particular configuration, no post-buckling strength was found in the room-temperature test. Therefore, the upper curve calculated from equation (1) gives the buckling strength and failure strength for uniform heating based on material deterioration with temperature. The lower curve gives the calculated bending load stress that produces buckling under the nonuniform-heating test condition (eq. (2)). The region between the curves then represents the amount of thermal stress that was calculated to be present in the tests. The circles give the failure-test results obtained from three beams. The results from two of the tests for non-uniform heating indicate that thermal stress in the beam reduced the maximum load. The maximum possible reduction was not large in the particular beam proportions tested, and it remains to be determined whether or not corresponding results will be obtained in beam proportions where the induced thermal stresses are a larger percentage of the beam buckling stress.

CYLINDER STRENGTH

Tests have been completed on 2024-T3 aluminum-alloy ring-stiffened circular cylinders (table I), and a program has been started with 17-7 PH stainless steel cylinders. The test setup is shown in figure 7. The cylinder is loaded in bending by the large weight cage acting through a linkage system. A quartz-tube lamp radiator constructed around the outside of the cylinder test section permits rapid heating of the cylinder skin with heat flowing into the rings primarily by conduction from the skin.

The effect of heating at different temperature rates on cylinder strength is shown in figure 8. The solid curve is the calculated bending strength of the ring-stiffened cylinder for uniform heating of both skin and rings and is based on the room-temperature test results of reference 1. The decrease in strength shown by the curve is caused by the change in elastic modulus at high temperatures.

Three nominally identical cylinders were loaded with two-thirds of the room-temperature failing load in bending and then heated to failure at temperature rates of 1° F/sec, 20° F/sec, and 90° F/sec. With the slowest temperature rate which corresponded essentially to a uniform heating test, the ring temperature followed the skin temperature very closely. For this case it would be expected that the buckling failure would be influenced mainly by the change in elastic modulus with temperature. The close agreement of the test at 1° F/sec with the curve for uniform heating checks the validity of such a calculation. For the two higher heating rates, ring temperatures lagged the skin temperature by a large amount. The lower curve in figure 8 is faired for these rapid heating tests and the gap between the curves indicates the effect of restrained expansion. Variations in cylinder diameter caused by restraint of thermal expansion of the skin by the rings were observed in the tests. The bulging between rings and circumferential compression stress produced by this restraint are the most probable causes for the reduction of strength of the two cylinders subjected to the high heating rates. For these particular cylinder proportions, temperature rates substantially less than the 20° F/sec would be required to avoid this reduction in strength.

The effect of changing the ring spacing is shown in figure 9 for a constant temperature rate of 90° F/sec. At room temperature the same value of failure stress is obtained for l/r equal to $1/2$ or greater. At a uniform elevated temperature a single calculated curve represents the strength of these cylinders. For l/r equal to $1/4$, the small ring spacing results in an increased bending strength for uniform heating conditions as shown by the top solid curve. The dashed curves are drawn to their respective test points for nonuniform heating at the high rate. The gap between the dashed curves and the corresponding solid curves is

a measure of the loss in bending strength caused by the restrained skin expansion. As the ring spacing increases, the loss in bending strength also increases.

It is believed to be significant that the mode of failure of these tests was the usual diamond buckle pattern and not a circumferential bulge such as would correspond to the eccentricity of the restrained skin. This behavior and the greater reduction in failure strength with increasing ring spacing suggest that the circumferential compression due to restrained skin expansion interacts more with the bending stress than does the eccentricity. This interaction becomes more serious as ring spacing is increased, inasmuch as the ratio of the actual to the critical circumferential compression stress increases.

CONCLUDING REMARKS

It may be concluded from these tests that thermal stresses will interact with bending load stresses to reduce the buckling load carried by a structure. Depending upon the mode of buckling, the thermal stresses may or may not affect the magnitude of the maximum load. In tests of structures where increases in load are required to produce deformation in the post-buckling range, no apparent effect of thermal stress on the failure load has been found; in structures which tend to deform with loss of load beyond buckling, tests indicate that a loss of strength due to thermal stress can be expected.

Langley Aeronautical Laboratory,
National Advisory Committee for Aeronautics,
Langley Field, Va., March 6, 1957.

REFERENCE

1. Peterson, James P.: Bending Tests of Ring-Stiffened Circular Cylinders. NACA TN 3735, 1956.

TABLE I

TEST RESULTS FOR 2024-T3 ALUMINUM-ALLOY RING-STIFFENED CYLINDERS
SUBJECTED TO RAPID HEATING AND BENDING LOADS

Cylinder: diameter, 19.16 in.; skin thickness, 0.0318 in. ± 1 percent.
Rings: $1\frac{1}{4}$ in. deep Z-section; 0.051 in. thick; area, 0.10 sq in.]

| Cylinder | Ring spacing, in. | Failing stress at room temperature, psi (a) | Applied stress, psi (a) | Nominal-skin-temperature rise rate, °F/sec | Maximum skin temperature at failure, °F | Ratio of E at failing temperature to E at room temperature | Temperature in rings at failure, °F (b) | Increase in diameter of ring, in. | Increase in diameter of skin at midspan, in. |
|----------|-------------------|---|-------------------------|--|---|--|---|-----------------------------------|--|
| I | $4\frac{3}{4}$ | ^c 17,500 | 11,800 | 1 | 599 | 0.68 | 487 to 596 | ----- | ----- |
| II | $4\frac{3}{4}$ | ^c 17,500 | 11,800 | 20 | 499 | .80 | 144 to 297 | 0.032 | 0.131 |
| III | $4\frac{3}{4}$ | ^c 17,500 | 11,800 | 90 | 489 | .81 | 80 to 214 | .007 | .113 |
| IV | $2\frac{3}{8}$ | ^d 20,700 | 14,300 | 90 | 550 | .74 | 80 to 260 | 0 | .124 |
| V | $9\frac{1}{2}$ | ^c 17,500 | 11,800 | 90 | 410 | .88 | 86 to 196 | ----- | ----- |

^aExtreme fiber bending stress.

^bMinimum and maximum temperatures measured over the ring cross sections.

^cStress obtained from test results for 7075-T6 cylinders of reference 1.

^dActual test.

STRESS-SHORTENING CURVES FOR VARIOUS STRUCTURAL COMPONENTS

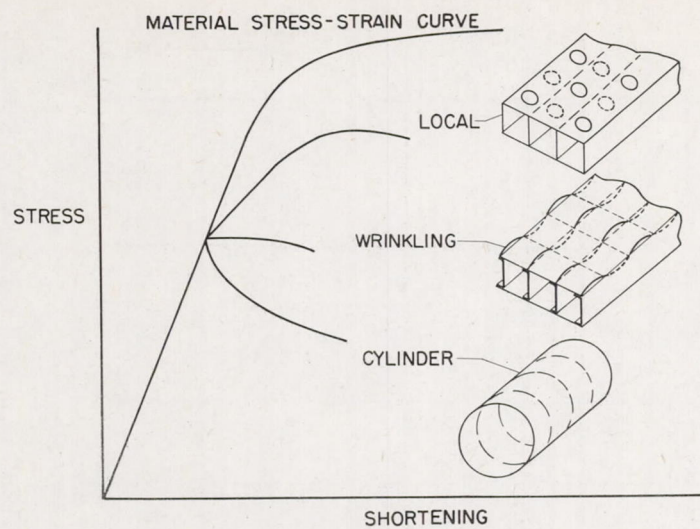
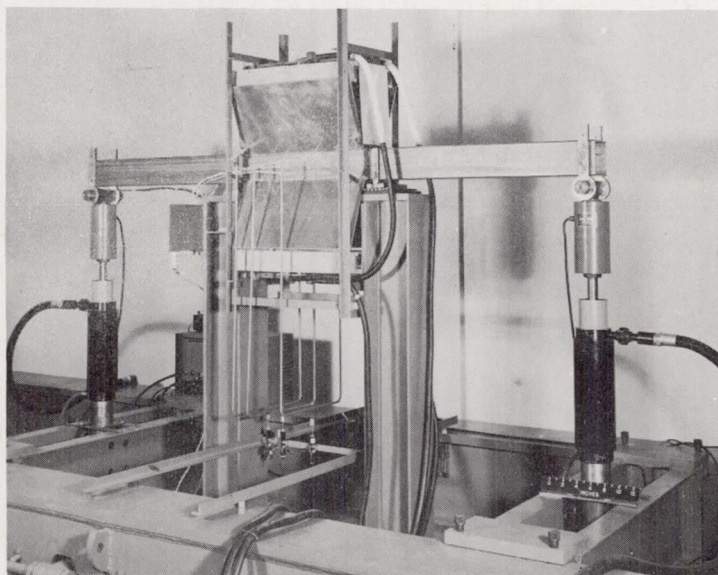


Figure 1

TEST SETUP FOR RAPID HEATING AND BENDING OF BEAMS



L-91930.1

Figure 2

TEMPERATURE DISTRIBUTION IN BEAM CROSS SECTION
2014-T6 ALUMINUM ALLOY; $\dot{T} \approx 100^\circ\text{F/SEC}$

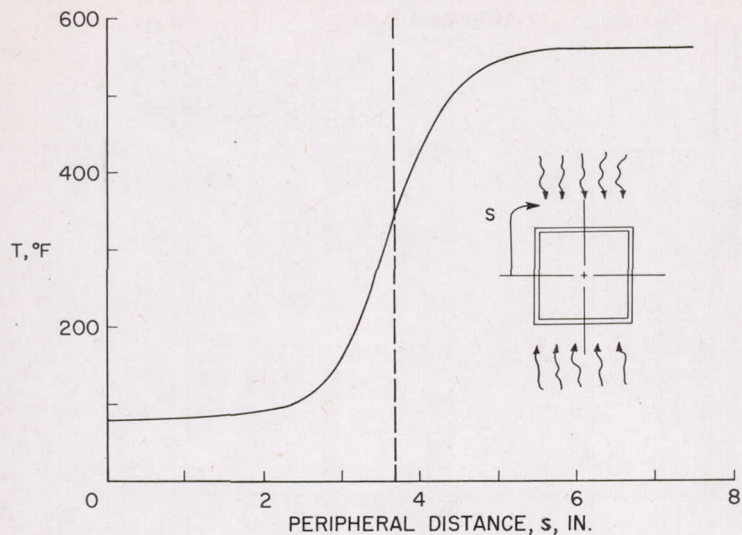


Figure 3

RAPID-HEATING EFFECTS ON BEAM BUCKLING
2014-T6 ALUMINUM ALLOY; $\dot{T} \approx 100^\circ\text{F/SEC}$

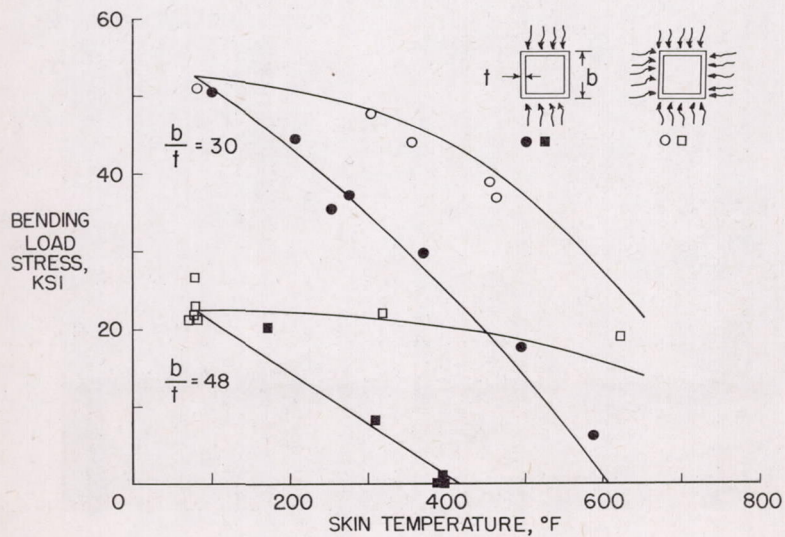


Figure 4

RAPID-HEATING EFFECTS ON BEAM FAILURE
2014-T6 ALUMINUM ALLOY; $\dot{T} \approx 100^\circ\text{F/SEC}$

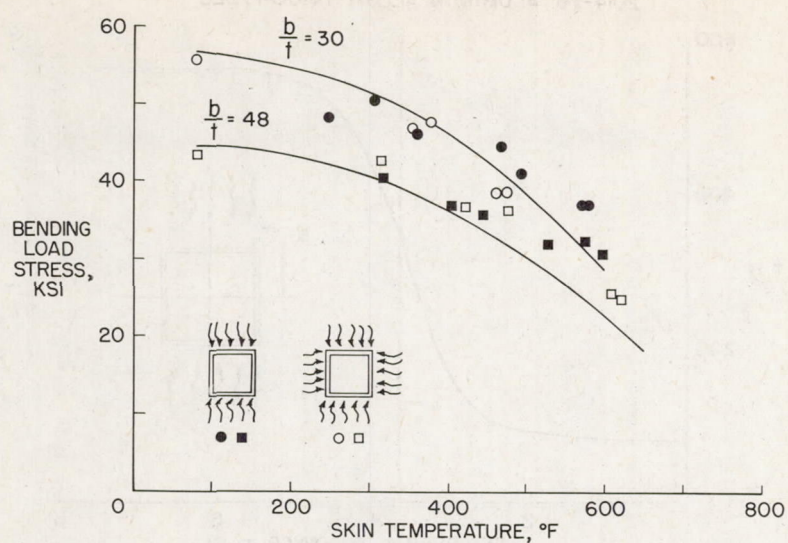


Figure 5

RAPID-HEATING EFFECTS ON BEAMS (WRINKLING MODE)
17-7 PH STAINLESS STEEL; $\dot{T} \approx 100^\circ\text{F/SEC}$

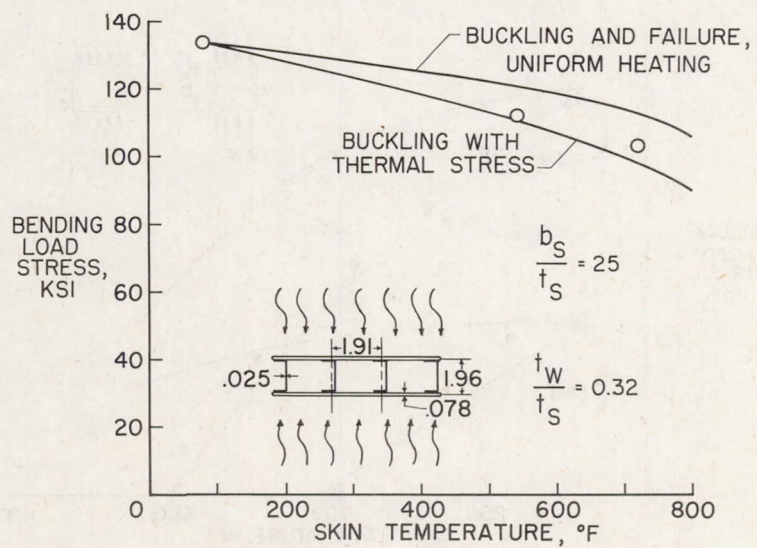


Figure 6

TEST SETUP FOR RAPID HEATING AND BENDING OF CYLINDERS

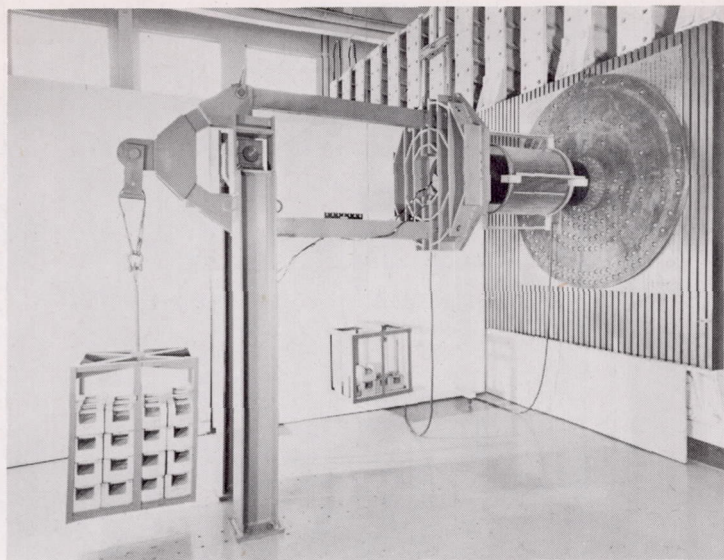


Figure 7 L-90701.1

RAPID-HEATING-RATE EFFECT ON RING-STIFFENED CYLINDER STRENGTH

$$2024-T3 \text{ ALUMINUM ALLOY}; \frac{l}{r} = \frac{1}{2}; \frac{r}{t} = 300$$

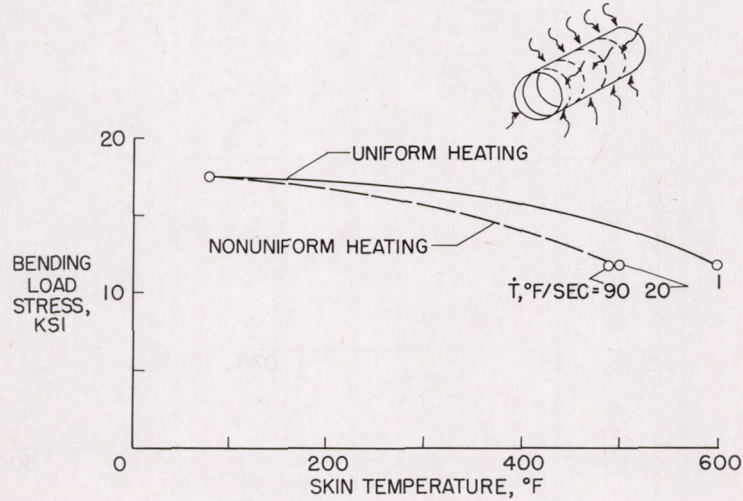


Figure 8

RING SPACING EFFECT ON STRENGTH OF RAPIDLY HEATED
RING-STIFFENED CYLINDERS

2024-T3 ALUMINUM ALLOY, $\frac{r}{t} = 300$, $\dot{T} = 90 \text{ }^{\circ}\text{F / SEC}$

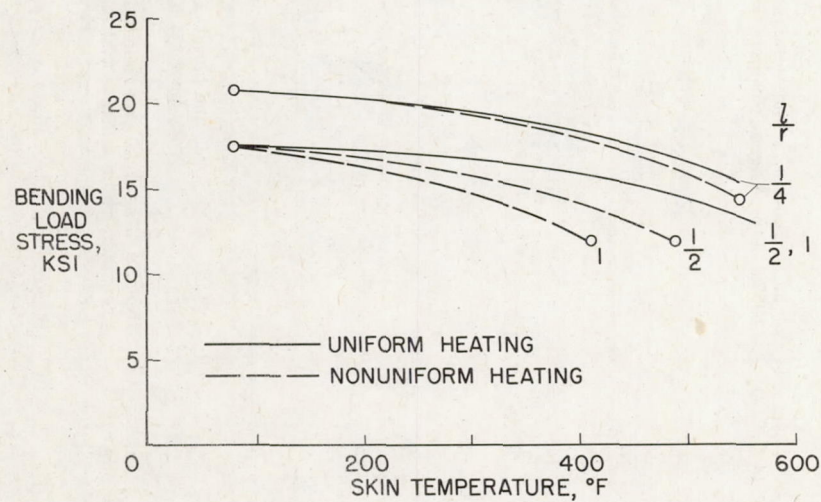


Figure 9